Bunch Compressor Beamlines for the TESLA and S-Band Linear Colliders

Paul Emma[†]

June 16, 1995

1 Introduction

A detailed design for a single stage beam bunch length compressor for both the TESLA and the S-Band Linear Collider (SBLC) is presented. Compression is achieved by introducing an energy-position correlation along the bunch with an *rf* section at zero-crossing phase followed by a short bending section with energy dependent path length (momentum compaction). The motivation for a wiggler design is presented and many of the critical single bunch tolerances are evaluated. A solenoid based spin rotator is included in the design and transverse emittance tuning elements, diagnostics and tuning methods are described. Bunch length limitations due to second order momentum compaction and sinusoidal *rf* shape are discussed with options for compensation. Finally, the disadvantages of bunch compression using a 180° arc are discussed.

2 Bunch Compressor Design Issues

The bunch compressor design is influenced by several criteria:

- *The compressor must reduce the damping ring extracted bunch length to the appropriate size.*
- *The system must perform a ~90° longitudinal phase space rotation so that damping ring extracted phase errors do not translate into linac phase errors which can produce large final focus beam energy deviations.*
- *The system must not significantly dilute the transverse emittances and should include tuning elements for correction.*
- *With its low energy and initially small energy spread, the bunch compressor is a convenient place to include solenoids for full control of the spin orientation.*
- *The compressor should be short, simple and as error tolerant as possible.*

3 Bunch Compressor Parameters

The equations for linear bunch compression are simple. The longitudinal linear phase space transformation through a simple bunch compressor constructed from an *rf* section followed by a bending section, in matrix notation, is

[†] Stanford Linear Accelerator Center, *Stanford, California*

$$\begin{bmatrix} z_1 \\ \delta_1 \end{bmatrix} = \begin{bmatrix} 1 & \alpha \\ 0 & 1 \end{bmatrix} \cdot \begin{bmatrix} 1 & 0 \\ k & 1 \end{bmatrix} \cdot \begin{bmatrix} z_0 \\ \delta_0 \end{bmatrix} , \tag{1}$$

where z_0 and z_1 are longitudinal particle positions within the bunch and δ_0 and δ_1 are fractional energy deviations ($\delta \equiv \Delta E/E_0$). The subscripts '0' and '1' refer to the locations of DR extraction and linac entrance, respectively. The momentum compaction parameter α (also referred to as R_{56} in TRANSPORT[1] notation) is defined here as the integral over the beam line axis, s, of the dispersion function, η, divided by the instantaneous bend radius, ρ.

$$\alpha \equiv \int \frac{\eta(s)}{\rho(s)} ds \tag{2}$$

The longitudinal 'focusing' parameter in (1), k, is defined using a linear approximation for the time dependence of an *rf* section with voltage V_0 and *rf* wavelength λ which is at a zero crossing phase.

$$\delta = \frac{eV_0}{E_0} \sin(2\pi z_0/\lambda) \approx \frac{2\pi e V_0}{\lambda E_0} z_0 \equiv k z_0 , \quad (z_0 << \lambda) \tag{3}$$

From (1), the rms bunch length at the entrance to the linac (for uncorrelated DR energy spread) is

$$\sigma_{z_1} = \sqrt{(1+\alpha k)^2 \sigma_{z_0}^2 + \alpha^2 \sigma_{\delta_0}^2} , \tag{4}$$

where σ represents the standard deviation of the subscripted coordinate. The minimum bunch length is achieved when $\alpha = -1/k$ which also decouples the linac phase ($\propto z$) from the DR phase. The momentum compaction is chosen to achieve the desired linac bunch length and the *rf* voltage is then given.

$$\alpha = -\frac{1}{k} = \sigma_{z_1}/\sigma_{\delta_0} , \quad eV_0 = -\frac{\lambda E_0}{2\pi\alpha} \tag{5}$$

The resulting energy spread at the linac entrance is approximately amplified by the inverse of the bunch compression factor.

$$\sigma_{\delta_1} = \sigma_{\delta_0} \sqrt{\left(\sigma_{z_0}/\sigma_{z_1}\right)^2 + 1} \approx \left(\sigma_{z_0}/\sigma_{z_1}\right) \cdot \sigma_{\delta_0} , \quad (\sigma_{z_1} << \sigma_{z_0}) \tag{6}$$

The energy-position correlation introduced along the bunch is insignificant. The correlation coefficient, $-1 < r < +1$, from (1) and (5) is

$$r \equiv \frac{\langle z_1 \delta_1 \rangle}{\sigma_{z_1} \sigma_{\delta_1}} = \frac{\sigma_{\delta_0}}{\sigma_{\delta_1}} . \tag{7}$$

The damping ring (DR) and initial linac parameters relevant for bunch compressor design are listed below in Table I[2].

Table I. Bunch compressor parameters for TESLA and SBLC. Emittance values represent those immediately after DR extraction.

parameter	symbol	unit	TESLA	SBLC
Energy	E_0	GeV	3.3	3.15
rms horizontal emittance	$\gamma\varepsilon_x$	mm-mrad	8.0	5.0
rms vertical emittance	$\gamma\varepsilon_y$	mm-mrad	0.13	0.20
rms DR bunch length	σ_{z0}	mm	8.9	4.0
rms DR energy spread	$\sigma_{\delta 0}$	%	0.094	0.115
rms linac bunch length	σ_{z1}	mm	0.6	0.3
rms linac energy spread	$\sigma_{\delta 1}$	%	1.39	1.53
rf wavelength	λ	mm	231	100
rf voltage	V_0	MV	190	192
rf gradient	G_{rf}	MV/m	25	17
length of *rf* section	L_{rf}	meters	7.6	11.3
momentum compaction	α	meters	0.64	0.26

4 Bunch Compressor Optics

A simple way to produce the necessary momentum compaction is with a chicane made of four horizontal bending magnets. A chicane of total length 24 m (13 m) for the TESLA (SBLC) design is possible, however, the peak dispersion required is large at 1.8 m (0.8 m). With 1.5% rms energy spread the horizontal beam size becomes very large at 27 mm (12 mm) and dipole field quality tolerances become tight. A more error tolerant design is achievable with a wiggler section[3] made up of N_p periods each with two bending magnets and two quadrupoles—one at each zero crossing of the dispersion function (see Fig. 5). If the bends are rectangular and each of length L_B with angle θ_B and separated by ΔL, and the quadrupoles alternately reverse sign to produce a phase advance per cell of ψ_x ($=\psi_y$), the momentum compaction, α_w, and the horizontal emittance growth due to synchrotron radiation (SR), $\Delta\gamma\varepsilon_x$, are given by[3]

$$\alpha_w = \frac{1}{4}\theta_B^2\left[N_p\left(2\Delta L + L_B\right) - \frac{1}{6}\left(2N_p + 1\right)L_B\right], \tag{8}$$

$$\Delta\gamma\varepsilon_x \approx \left(1.25\times10^{-8}\,\mathrm{m}^2\cdot\mathrm{GeV}^{-6}\right)\cdot E_0^6 N_p \frac{|\theta_B|^5}{L_B^2}\frac{\left(\Delta L + L_B\right)}{|\sin\psi_x|}. \tag{9}$$

By setting the necessary momentum compaction[4] and choosing a horizontal SR emittance dilution of 1-2%, a dipole field strength of ~15 kG, and roughly minimizing dipole magnet length and peak dispersion, the following wiggler designs, Table II,

were developed for the two colliders. With $|\sin\psi_x|^{-1}$ minimized at $\psi_x = \pi/2$, the number of periods is chosen so that each dipole at peak dispersion has an opposing dipole separated by π in betatron phase advance so that all orders of dispersion generated by equal multipole field components cancel. The peak horizontal beam size in the wiggler is 4.3 mm (2.6 mm) in TESLA (SBLC). The beta and dispersion functions and a schematic beamline layout of the TESLA wiggler (including a 12 meter, 8 cavity TESLA superconducting *rf* module) are plotted in Fig. 1.

Table II. Wiggler design parameters for TESLA and SBLC using parameters of Table I (NOTE: All non-correction quadrupoles in the entire beamline are of length 15 cm and pole tip radius 1 cm).

parameter	symbol	unit	**TESLA**	**SBLC**
momentum compaction[4]	α_w	meters	0.600	0.260
dipole magnet length	L_B	meters	2.0	1.5
bend-to-bend separation	ΔL	meters	3.22	2.50
bend angle / dipole	θ_B	degrees	16.0	12.0
total length	$L_{\rm tot}$	meters	47	36
maximum x-dispersion	$\eta_{\rm max}$	mm	308	170
SR x-emittance dilution	$\Delta\varepsilon_x/\varepsilon_{x0}$	%	1.8	0.7
dipole magnetic field	B_0	kG	15.37	14.67
quad. pole tip fields — F (D)	B_0	kG	2.0 (1.7)	
number of periods	N_p	—	4	4
phase advance per period	ψ_x	degrees	90	90

From this point on the SBLC design will not be followed in such detail. The two colliders may use very similar bunch compressor beamlines for either e^- or e^+.

5 Peripheral Sections and the Full Beamline

In addition to the primary function of bunch compression, the beamline described here also includes sections for spin rotation, cross-plane coupling correction, and phase space diagnostics. This section describes these modules (for reference, the entire beamline is depicted in Fig. 4 and 5).

I. Spin Rotator

Using the TESLA damped vertical emittance, it can be shown[5] that for a chicane type "half serpent" $\pi/2$ spin rotator[6] constructed from horizontal and vertical bending magnets, and for <2% SR vertical emittance dilution, the relationship between the length of the bending magnets and the beam energy is discouraging.

$$L[\mathrm{m}] > 30 \cdot E[\mathrm{GeV}] \tag{10}$$

Even at 3.3 GeV the dipoles are ~100 meters long. Therefore a spin rotator based on superconducting solenoids is proposed prior to bunch compression. Since the damped

beam is flat ($\varepsilon_y / \varepsilon_x < 1$) the cross-plane coupling induced by the solenoids must be compensated. This is achieved by rotating the spin by $\pi/2$ around the longitudinal axis with a pair of $\pi/4$ solenoids separated by a 'reflector' beamline which causes the solenoid pair's coupling to cancel while their spin precession adds. In this way the solenoid coupling is always canceled regardless of the solenoid settings as long as the solenoid pairs have equal strength (±2%). By separating two such solenoid pair systems with a $\pi/2$ spin rotation around the vertical axis (*i.e.* an arc of total bend angle $\theta = \pi/2a\gamma$) full arbitrary control of the spin orientation is possible. The focusing effect of the solenoids is corrected with four matching quadrupoles per paired solenoid section. The matching quadrupoles are positioned between the paired solenoid sections and the central arc (Fig. 2). A similar solenoid rotator system is more fully described in reference 6. At ~0.1% rms DR energy spread the emittance dilution due to chromatic-coupling of the four solenoids together at maximum field is negligible at 0.7%. The parameters of the spin rotator system are given in Table III.

Table III. Spin rotator parameters for TESLA (or approx. for SBLC).

parameter	symbol	unit	**TESLA**
effective solenoid length	L_{sol}	meters	2.275
maximum solenoid field	B_z	kG	±38.0
total arc bend angle	θ	degrees	12.0
total length of rotator system	L_{tot}	meters	52
number of dipole magnets (12° arc)	N_{dipole}	—	4
dipole field	B_0	kG	6.1
SR x-emittance dilution	$\Delta\varepsilon_x/\varepsilon_{x0}$	%	$\sim 1\times10^{-3}$
momentum compaction of all arcs	α_a	m	0.02
chromatic ε_y dilution ($\sigma_{\delta 0}$ = 0.1%)	$\Delta\varepsilon_y/\varepsilon_{y0}$	%	0.7
chromatic ε_y dilution ($\sigma_{\delta 0}$ = 0.2%)	$\Delta\varepsilon_y/\varepsilon_{y0}$	%	4.6
chromatic ε_y dilution ($\sigma_{\delta 0}$ = 0.3%)	$\Delta\varepsilon_y/\varepsilon_{y0}$	%	10.9

It is also desirable to include a wire scanner (or profile monitor) near one of the dispersion peaks in the 12° arc in order to monitor DR energy spread. The horizontal betatron beam size is ~75 μm while the dispersive beam size is ~200 μm. Furthermore, DR energy pre-collimation may be performed at the other peak. Similarly, DR bunch length measurements and collimation may be performed in the wiggler where the betatron and dispersive beam sizes are similarly favorable. It should be noted that momentum compaction of the rotator arcs has no significant effect on the longitudinal phase space.

II. Coupling Correction Section

In order to empirically correct anomalous cross-plane coupling due to either damping ring extraction errors or spin rotator errors, a skew correction section (SCS) is included immediately following the final rotator solenoid. The system is constructed from four

small skew quadrupoles with zero nominal strength. The first and second skew quadrupoles are separated by betatron phases of $\Delta\psi_x = \Delta\psi_y = \pi/2$. This is also true for the third and fourth skew quadrupoles. The second and third are separated by $\Delta\psi_x = \pi$, $\Delta\psi_y = \pi/2$ such that the four skew quadrupoles orthogonally control the four coupling coefficients in the beam: $\langle x'y\rangle$, $\langle xy'\rangle$, $\langle xy\rangle$ and $\langle x'y'\rangle$, respectively. The four skew corrections are actually orthonormal in that the emittance sensitivity to each skew quadrupole is designed to be a constant (*i.e.* $\beta_x\beta_y$ is equal at each skew quadrupole). Fig. 3 shows the beta functions and beamline of the SCS. The coupling correction is applied by sequentially minimizing the measured vertical emittance (see subsection III) with each skew quadrupole. As the skew elements take on some strength the system loses the feature of perfect orthonormality due to the slight effect of the skew elements on the phase advance and beta functions of the ideal system. Some reiteration of the tuning may be required for large coupling corrections (*e.g.* $\varepsilon_y/\varepsilon_{y0} > 2$). The relative emittance increase for one thin skew quadrupole of focal length f at beta functions of $\beta_x\beta_y$ is

$$\frac{\varepsilon_y}{\varepsilon_{y0}} = \sqrt{1+\frac{\varepsilon_{x0}}{\varepsilon_{y0}}\frac{\beta_x\beta_y}{f^2}} \qquad (11)$$

With skew quadrupoles of 10 cm length, ±1 kG pole tip fields and 1 cm radii, a factor of ~2 emittance increase can be corrected per skew quadrupole.

III. Diagnostic Section

It is important to provide measurement capability after the bunch compressor so that the beam emittance and matching can be monitored and corrected before entrance into the main linac. Following the wiggler section is a simple set of three FODO cells with phase advance per cell of $\Delta\psi_x = \Delta\psi_y = 45^\circ$ (see Fig. 4). By placing four wire scanners[7] near the vertical focusing quadrupoles the ideal four-wire scanner phase sampling is available to make high precision emittance and beta function measurements in each plane. The nominal rms beam size at the scanners is chosen as 15 μm (19 μm) vertically and 80 μm (65 μm) horizontally for TESLA (SBLC). A matched beam is easily identified since in this case the beam sizes per plane are identical at each of the four wire scanners. The cross-plane coupling in the beam is not fully measurable with this section. However, by simply minimizing the vertical emittance (flat beam) with the four SCS skew quadrupoles all coupling can be corrected (with some iteration necessary in extreme cases). A direct measurement capability is achievable, if desired, by using six wire scanners with phase advances similar to the SCS described above[8].

IV. Compressor RF Section

The energy-position correlation is introduced with one 12 meter superconducting TESLA accelerating module with eight cavities each of 1.035 meter length with gradient of 25.0 MV/m in order to produce the necessary 207 MV for full bunch compression.

V. The Combined Beamline

The four sections described thus far (spin rotator, coupling correction, bunch compressor and diagnostics) are combined using various appropriate matching quadrupoles to preserve the periodic beta functions in the various FODO cells. Fig. 4 shows the beta and dispersion functions of the combined system. The combined system floorplan is laid out in Fig. 5 (quadrupoles not shown). The system, including the 3.1 meter spin rotator bump, should fit inside a 5 meter diameter tunnel. The angle of the first arc may be reduced and the angle of the third arc equally increased if it is necessary to horizontally displace the outgoing beamline relative to the incoming one. It is only necessary that the 12° arc remain fixed (for 3.3 GeV) so that the electron or positron spin orientation is fully controllable over a sphere.

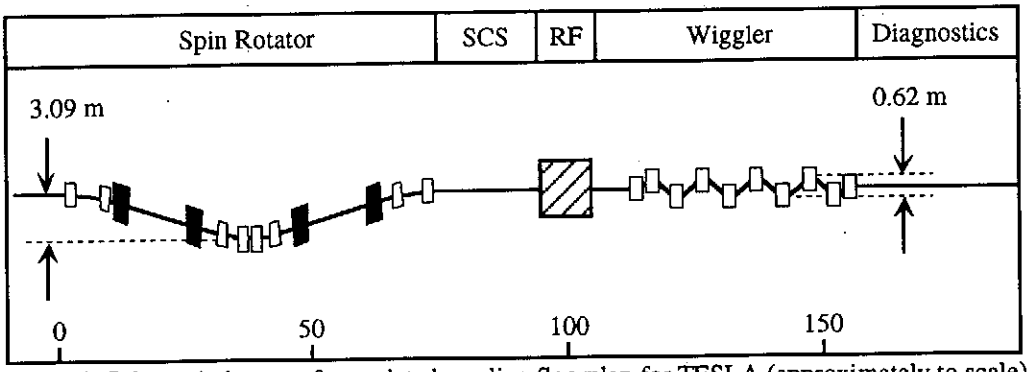

Fig. 5. Schematic layout of complete beamline floorplan for TESLA (approximately to scale). Solenoids are in black, dipoles are in white and the *rf* module is cross-hatched (quadrupoles not shown).

VI. Chromaticity and Non-linearities

The entire beamline has been tracked with 3rd order TRANSPORT[1] and TURTLE[9] to evaluate chromatic effects (there are no sextupoles in the beamline). Table IV lists the relative horizontal and vertical emittance increase, the final energy spread and the final rms bunch length as function of the initial DR rms bunch length for 3000 Gaussian distributed particles including the effect of sinusoidal *rf* and higher order optical aberrations. The emittance is insensitive, however the final bunch length can be quite sensitive due to the sinusoidal character of the *rf* (see section 9).

Table IV. Sensitivity of emittance, final energy spread and final bunch length to variations in DR bunch length, including sinusoidal *rf* and higher order optical aberration. All solenoids are at maximum field. The *rf* voltage (207 MV) was adjusted to minimize the final bunch length at the nominal initial value of 8.9 mm but was not optimized for the other various DR bunch lengths.

σ_{z0} /mm	σ_{z1} /mm	$\sigma_{\delta 1}$ /%	$\Delta\varepsilon_x/\varepsilon_{x0}$ /%	$\Delta\varepsilon_y/\varepsilon_{y0}$ /%
0	0.56	0.094	0	0
4.50	0.59	0.76	0.2	0.1
6.75	0.61	1.12	0.4	0.4
8.90	0.68	1.48	0.7	0.8
11.2	0.85	1.83	1.0	1.3
13.5	1.15	2.14	1.3	1.7

18.0	2.30	2.71	1.9	2.6

6 Single Bunch Tolerances

The large energy spread and strong bending of the wiggler present some challenges for transverse emittance preservation, especially in the vertical plane. Several important tolerances are examined below. Table V evaluates these tolerances. The next section will deal with tuning strategies and tuning elements to open these tolerances.

I. Dipole Magnet Roll Tolerances

A rolled dipole magnet introduces vertical dispersion which, if not corrected, will chromatically filament in the main linac and dilute the vertical emittance, $\Delta\varepsilon_y/\varepsilon_{y0}$. The roll angle tolerance, ϕ, for a single dipole magnet of bend angle θ_B and vertical beta function β_y is (not including effects of the offset trajectory beyond the dipole)

$$|\phi| < \frac{1}{\sigma_\delta|\theta_B|}\sqrt{\frac{2\varepsilon_{y0}}{\beta_y}\left(\frac{\Delta\varepsilon_y}{\varepsilon_{y0}}\right)} \quad . \tag{12}$$

II. Quadrupole and Sextupole Field Components in Dipoles

A quadrupole (sextupole) field component in a dipole with horizontal dispersion, η_x, and horizontal beta function, β_x, will dilute the horizontal emittance through the generation of first (second) order horizontal dispersion. The tolerance for the normal quadrupole (sextupole) field component, b_1 (b_2), with respect to the dipole field, b_0, measured at a radius r_0, is then (Gaussian energy spread assumed)

$$\left|\frac{b_1}{b_0}\right| < \frac{1}{|\theta_B|}\left(\frac{r_0}{\eta_x\sigma_\delta}\right)\sqrt{\frac{2\varepsilon_{x0}}{\beta_x}\left(\frac{\Delta\varepsilon_x}{\varepsilon_{x0}}\right)}, \qquad \left|\frac{b_2}{b_0}\right| < \frac{1}{|\theta_B|}\left(\frac{r_0}{\eta_x\sigma_\delta}\right)^2\sqrt{\frac{\varepsilon_{x0}}{\beta_x}\left(\frac{\Delta\varepsilon_x}{\varepsilon_{x0}}\right)} \quad . \tag{13}$$

The symmetry of the wiggler optics introduces a strong cancellation of these two effects if the dipole field errors are similar for all magnets. This tolerance, when applied to the wiggler dipoles, can therefore be considered as a constraint on the field uniformity over the eight inner wiggler dipoles (the first and tenth have near zero dispersion).

III. Qadrupole Magnet Misalignments

A misaligned quadrupole will generate vertical and/or horizontal dispersion. The misalignment tolerance, $\Delta_{x,y}$, for a quadrupole of focal length f is

$$|\Delta_{x,y}| < \frac{|f|}{\sigma_\delta}\sqrt{\frac{2\varepsilon_{x,y0}}{\beta_{x,y}}\left(\frac{\Delta\varepsilon_{x,y}}{\varepsilon_{x,y0}}\right)} \quad . \tag{14}$$

IV. Quadrupole Roll Errors

A rolled quadrupole in a non-dispersive section will couple the beams while a rolled quadrupole in a dominantly dispersive section will generate vertical dispersion. The roll tolerance for a quadrupole of focal length f in both cases of $\eta_x = 0$ and $\eta_x \neq 0$, is

$$|\phi(\eta_x = 0)| < |f| \sqrt{\frac{2}{\beta_x \beta_y} \frac{\varepsilon_{y0}}{\varepsilon_{x0}} \left(\frac{\Delta\varepsilon_y}{\varepsilon_{y0}} \right)}, \qquad |\phi(\eta_x \neq 0)| < \frac{|f|}{|\eta_x| \sigma_\delta} \sqrt{\frac{2\varepsilon_{y0}}{\beta_y} \left(\frac{\Delta\varepsilon_y}{\varepsilon_{y0}} \right)} \quad . (15)$$

Table V lists a range of roll tolerances with the tightest tolerance on one of the matching quadrupoles just after the *rf* section and also on the center 12° arc quadrupole (see Fig. 1 and 2). The loosest tolerances are on the wiggler quadrupoles which are weak.

V. Spin Rotator Tolerances

There are also tolerances on the difference of the field strengths between the paired solenoids and also on the absolute gradient of the eight quadrupoles which make up the reflector beamline between the paired solenoids. These tolerances have been evaluated with tracking and are included in Table V below which evaluates the tolerances discussed in this section. These tolerances assume no correction (see next section). The reflector beamline quadrupole gradient tolerances are evaluated at the maximum solenoid field and vary over the eight quadrupoles. The tightest of the eight are the two quadrupoles which are most centered between the paired solenoids.

VI. Phase Tolerance of Compressor RF

If the phase, φ_{rf}, of the compression *rf* were to deviate from the zero crossing this energy offset will advance or delay the phase of the bunch as it enters the linac and upset the collision timing at the interaction point (IP). The tolerance of the *rf* phase for IP stability of $|\langle z_1 \rangle| < \sigma_{z1}/n$ (*e.g.* n = 3) is given by (see Table V)

$$|\varphi_{rf}| < \left(\frac{\sigma_{z_1}}{n} \right) \frac{E_0}{\alpha_w e V_0} \quad . \qquad (16)$$

Table V. Single element tolerances for TESLA wigglers and spin rotators for <2% emittance dilution or $|\langle z_1 \rangle| < \sigma_{z1}/3$ IP longitudinal stability (no correction assumed). SBLC will be similar with somewhat less difficult tolerances due to its increased vertical emittance and shorter DR bunch length.

tolerance	symbol	unit	**TESLA**
wiggler dipole magnet roll tolerance	$\|\phi\|$	μrad	80
quad. field in wiggler dipole (r_0=20 mm)	$\|b_1/b_0\|$	—	4.0×10^{-5}
sext. field in wiggler dipole (r_0=20 mm)	$\|b_2/b_0\|$	—	1.4×10^{-4}
F-quad. x-misalignment tolerance	$\|\Delta_x\|$	μm	460
D-quad. y-misalignment tolerance	$\|\Delta_y\|$	μm	70
Quadrupole roll tolerance range	$\|\phi\|$	mrad	3.5 - 14
Paired solenoid field difference tolerance	$\|\Delta b_z\|/B_{z\text{-max}}$	%	2
reflector quad. grad. tol. range (max. sol.)	$\|\Delta G\|/G_0$	%	0.4 - 1.7
compression *rf* phase stability tol. (n=3)	$\|\varphi_{rf}\|$	degrees	0.33

The roll tolerances are quite tight and probably difficult to achieve. However, these tolerances can be opened by an order of magnitude by including small normal and skew quadrupoles of zero nominal field to be used for dispersion correction.

7 Tuning Elements and Schemes

I. Dispersion Correction

In order to correct for the inevitable errors such as those listed above, several tuning elements have been added to the beamline. The most needed corrections will likely be to the dispersion through the wiggler due to quadrupole misalignments and dipole roll and field errors. Cross-plane coupling may arise due to gradient errors in the reflector beamline and a mis-matched beta function may occur anywhere in the beamline. Two small skew quadrupoles ($L = r_0 = 5$ cm) of zero nominal field are located at high dispersion in the wiggler—one in front of dipole #4 and the other at #6 (see Fig. 5) so that they are separated by $\pi/2$ in betatron phase advance. These two elements span the space for the correction of anomalous vertical dispersion and its slope and generate no significant coupling due to the large ratio: $(\eta_x \sigma_\delta)^2/\beta_x \varepsilon_x \sim 10^3$. At pole tip field of $B_0 = \pm 1.0$ kG these elements, with focal length f, can each correct an emittance dilution due to anomalous vertical dispersion, including linac filamentation, of

$$\frac{\Delta\varepsilon_y}{\varepsilon_{y0}} = \frac{\eta_x^2}{f^2}\frac{\beta_y \sigma_{\delta_1}^2}{2\varepsilon_{y0}} \approx 160 \qquad (17)$$

(a field of $B_0 = \pm 0.01$ kG will produce a 2% emittance change). With this correction range available the dipole roll and vertical quadrupole misalignment tolerances can be effectively scaled up by more than an order of magnitude. Similarly, two small normal quadrupoles are located up-beam of dipoles #3 and #5 to correct horizontal dispersion and its slope. These quadrupoles can correct a relative horizontal emittance increase of ~2.5. Two more skew quadrupoles ($L = 10$ cm, $r_0 = 1$ cm) are also located in front of dipoles #2 and #4 in the 12° arc for vertical dispersion correction in the 12° arc for up to a factor 10 in emittance growth. Any anomalous dispersion at this point can not be compensated in the wiggler tuning since the energy spreads in each section have different sources.

II. Coupling Correction

The cross-plane coupling correction has already been described. The four orthonormal skew quadrupoles are capable of fully correcting all linear coupling from whatever source in the compressor beamline.

III. Beta Matching

Many matching quadrupoles exist throughout the beamline which may be used to correct matching errors in the beam before it enters the main linac. Primarily the two

sets of solenoid compensation quadrupoles around the 12° arc should provide correction.

IV. Tuning Schemes

The various emittance dilution mechanisms may be separated in practice by switching off solenoids while dispersion matching and/or switching off the *rf* while beta matching and correcting coupling. Tuning is guided by emittance and beta function measurements with the wire scanners in the diagnostic section. A possible tuning scenario may proceed as follows:

- *Set the solenoids for the desired spin orientation.*
- *Switch off the compressor* rf.
- *Empirically minimize the vertical emittance with the four skew quadrupoles in the SCS—if the emittance is reduced by a factor of more than ~1.5, reiterate.*
- *Match the beam on the wire scanners in each plane by adjusting one or more of the matching quadrupoles around the 12° arc (empirically or by calculation).*
- *Switch on the compressor* rf *and minimize the emittance per plane with the wiggler skew and normal correction quadrupoles—linear combinations can be used which are exactly orthogonal* (η *and* $\eta\alpha + \eta'\beta$).
- *Try to further minimize the vertical emittance, if necessary, by adjusting the 12° arc skew quadrupoles in appropriate linear combinations (probably a small effect).*

8 Second Order Momentum Compaction

Numerical evaluation of the effects described in the following sections are summarized in Table VI. An analytical description concerning bunch length limitations and DR extraction phase stability tolerances precedes this.

I. Bunch Length Limitations

The compression arguments presented thus far are limited to linear effects. In fact the bunch is not infinitely compressible and at some point second order momentum compaction limits the achievable bunch length. Including the second order momentum compaction, α_2, the linac bunch position of a particle has a quadratic dependence on its DR bunch position.

$$z_1 = [\alpha + \alpha_2\delta_0]\delta_0 + (1 + k[\alpha + \alpha_2\delta_0])z_0 + \alpha_2 k^2 z_0^2 \approx \alpha\delta_0 + \alpha_2 k^2 z_0^2 \qquad (18)$$

The approximation made at the right of (18) is possible since $\alpha_2\delta_0 << \alpha$ and $k = -1/\alpha$. For a wiggler, the approximate relationship between the second and first order momentum compaction is[10,11]

$$\alpha_2 \approx -\frac{3}{2}\alpha \ . \qquad (19)$$

For a DR bunch length distribution which is Gaussian (*i.e.* $\langle z_0^4 \rangle = 3\langle z_0^2 \rangle^2$), the linac rms bunch length using (18) and (19) is

$$\sigma_{z_1}^2 \approx \langle z_1^2 \rangle - \langle z_1 \rangle^2 = \alpha^2 \sigma_{\delta_0}^2 + \frac{9}{2} \cdot \frac{\sigma_{z_0}^4}{\alpha^2} \quad . \tag{20}$$

As α is reduced in order to compress the bunch toward zero, the second term of (20) begins to dominate the final bunch length. Using the linear relation $\alpha = \sigma_{z1\text{-lin}}/\sigma_{\delta 0}$, the minimum achievable bunch length is, by differentiating (20) with respect to the linear bunch length$\sigma_{z1\text{-lin}}$,

$$\sigma_{z_{1-\min}} = \sqrt{3\sqrt{2}\sigma_{\delta_0}}\,\sigma_{z_0} \quad , \quad \text{(at linear } \sigma_{z_1} \text{ of : } \sqrt{\frac{3\sigma_{\delta_0}}{\sqrt{2}}}\sigma_{z_0}) \quad . \tag{21}$$

Fig. 7 below shows a plot of the 'second order' rms bunch length (including second order momentum compaction) vs. the linear 'design' bunch length.

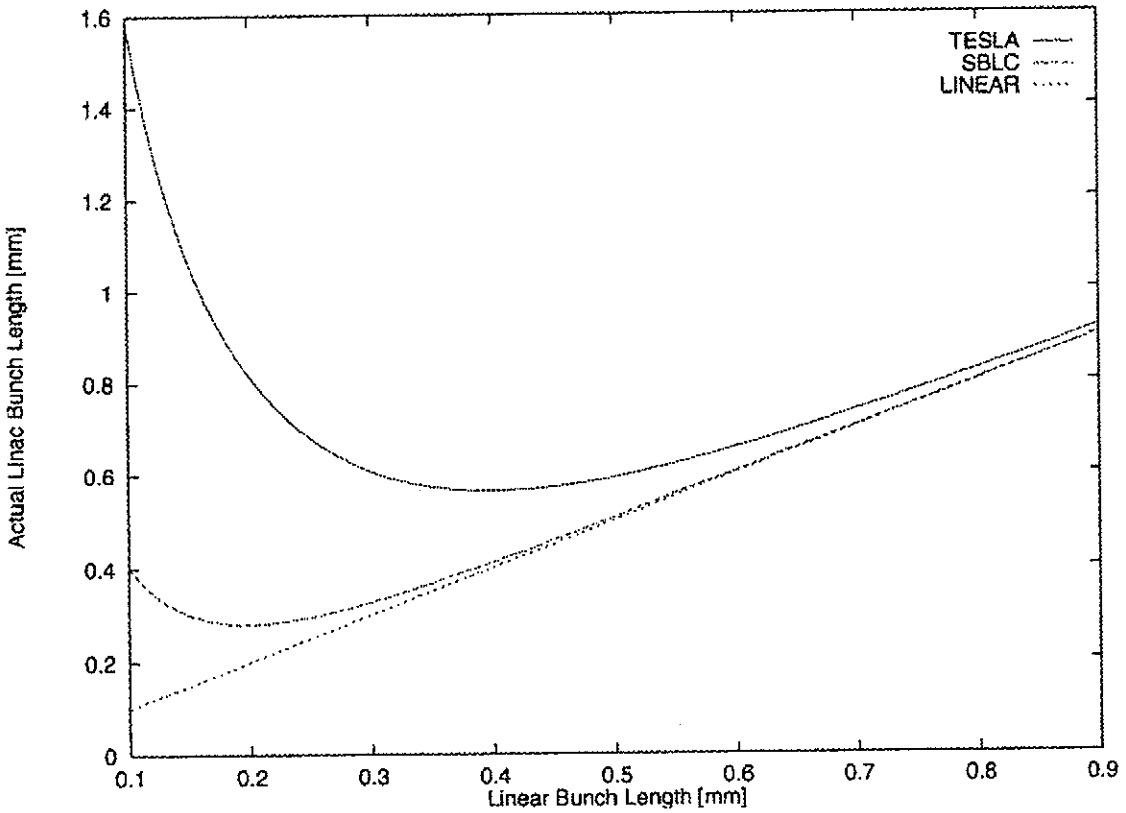

Fig. 7. Calculated rms bunch length, including second order momentum—using (20) above, vs. linear 'design' bunch length for TESLA and SBLC. The DR bunch distribution is taken as a Gaussian here. The straight line is a linear model.

II. Damping Ring Extraction Phase Jitter Effects

In addition to limiting the achievable bunch length, the second order momentum compaction also gives rise to a quadratic linac "phase" dependence on DR "phase" — see eq. (18). Thus, DR extraction "phase" errors, $\langle z_0 \rangle$, will transform into final focus (ff) energy deviations roughly depending on the mean accelerating *rf* phase in the main linac, $\langle \varphi \rangle$ (=0 at *rf* crest). For small "phase" errors, $\langle z_1 \rangle << \lambda$, and including only the *rf* curvature in the main linac, final focus energy deviations, $\langle \delta_{ff} \rangle$, can be approximated by

$$\langle \delta_{ff} \rangle \sim -\frac{2\pi \tan\langle \varphi \rangle}{\lambda} \cdot \langle z_1 \rangle \quad . \tag{22}$$

The DR extraction "phase" jitter tolerance is then, using (18) and (19),

$$|\langle z_0 \rangle|_{tol} < \sqrt{\frac{|\langle \delta_{ff} \rangle|_{tol} \lambda \alpha}{3\pi |\tan\langle \varphi \rangle|}} \quad . \tag{23}$$

The necessary stability of the longitudinal beam position at the interaction point (IP) also sets a tolerance on DR "phase" jitter. Using (18) the DR "phase" jitter tolerance for fraction bunch position IP stability of $|\langle z_1 \rangle| < \sigma_{z1}/n$ (*e.g.* n =3) is

$$|\langle z_0 \rangle|_{tol} < \sqrt{\frac{2\alpha\sigma_{z_1}}{3n}} \quad . \tag{24}$$

The magnitudes of these effects for each collider are summarized in Table VI after the next section which deals with similar effects due to the sinusoidal character of the compressor *rf*.

9 Effects of Sinusoidal Compressor RF

The bunch length is also limited by the sinusoidal character of the compressor *rf*. Including the 3rd order term of the $\sin(z_0)$ expansion in (3) and not including the second order momentum compaction, the bunch position of a particle in the linac, for full compression where $k = -1/\alpha$, is

$$z_1 \approx \alpha\delta_0 + \frac{1}{6}\left(\frac{2\pi}{\lambda}\right)^2 \cdot z_0^3 \quad , \tag{25}$$

and for a DR bunch length distribution which is initially gaussian (*i*.e. $\langle z_0^6 \rangle = 15\langle z_0^2 \rangle^3$), the rms bunch length is calculated as in (20).

$$\sigma_{z_1}^2 \approx \alpha^2\sigma_{\delta_0}^2 + \frac{5}{12}\left(\frac{2\pi}{\lambda}\right)^4 \cdot \sigma_{z_0}^6 \tag{26}$$

In this case the minimum achievable bunch length is in the direction α ->0. The DR extraction "phase" jitter tolerance, as in (23), due to the sinusoidal *rf* is also given by (25). Using (22) and $\langle z_1 \rangle$ from (25),

$$|\langle z_0 \rangle|_{tol} < \frac{\lambda}{2\pi}\left(\frac{6|\delta_{ff}|}{|\tan\langle \varphi \rangle|}\right)^{1/3} \quad . \tag{27}$$

Required IP longitudinal stability, as in (25), sets a DR "phase" jitter tolerance, using (25), of

$$|\langle z_0 \rangle|_{tol} < \left(\frac{6\sigma_{z_1}}{n}\left[\frac{\lambda}{2\pi}\right]^2\right)^{1/3} \quad . \tag{28}$$

Bunch length limitations and DR phase jitter tolerances for both second order momentum compaction and sinusoidal *rf* effects are summarized below in Table VI for both colliders. It can be shown that the two non-linear bunch length limitations discussed above approximately add in quadrature. The net rms bunch length, including both effects, is listed at the end of the table. Note, with these non-linear effects the rms bunch length results are somewhat dependent on the initial DR extracted bunch distribution—taken as a Gaussian here.

Table VI. Bunch length limits and DR phase jitter tolerances, due to second order momentum compaction and sinusoidal compressor *rf* each taken in isolation, for TESLA and SBLC using Table I parameters. The DR extracted bunch length distribution is taken as a Gaussian for these calculations.

parameter	symbol	unit	**TESLA**	**SBLC**
linac *linear* bunch length	σ_{z1}	mm	0.56	0.30
linac *rf* frequency	f_{rf}	GHz	1.3	3.0
linac mean acc. phase	$\langle\varphi\rangle$	degrees	3.3	2
The following include the effect of second order momentum compaction only.				
linac rms 2nd order bunch length	σ_{z1}	mm	0.63	0.33
min. 2nd order linac bunch length	$\sigma_{z1\text{-min}}$	mm	0.56	0.28
DR "phase" tol –> $\lvert\langle\delta_{ff}\rangle\rvert < 0.1\%$	$\lvert\langle z_0\rangle\rvert_{tol}$	mm (deg)	16 (26)	8.9 (32)
DR "phase" tol –> $\lvert\langle z_1\rangle\rvert/\sigma_{z1} < 1/3$	$\lvert\langle z_0\rangle\rvert_{tol}$	mm (deg)	9.2 (14)	4.2 (15)
The following include the effect of the sinusoidal rf *only.*				
linac rms sinusoidal bunch length	σ_{z1}	mm	0.65	0.34
min. rms sinusoidal linac b.l.	$\sigma_{z1\text{-min}}$	mm	0.34	0.16
DR "phase" tol –> $\lvert\langle\delta_{ff}\rangle\rvert < 0.1\%$	$\lvert\langle z_0\rangle\rvert_{tol}$	mm (deg)	17 (27)	8.8 (32)
DR "phase" tol –> $\lvert\langle z_1\rangle\rvert/\sigma_{z1} < 1/3$	$\lvert\langle z_0\rangle\rvert_{tol}$	mm (deg)	12 (18)	5.3 (19)
The following includes both of the above non-linear bunch length limitations.				
linac rms bunch length	σ_{z1}	mm	0.70	0.36

The rms linac bunch length will be ~20% larger than the linear design value without compensation. The DR phase jitter tolerances in Table VI are quite loose and should not present a problem for final focus energy and IP longitudinal stability. Figure 8 below shows the longitudinal phase space after the full compressor beamline of TESLA. This is generated with tracking using TURTLE[9] which includes second order momentum compaction and sinusoidal *rf*. Note these results are sensitive to the actual DR bunch length distribution—assumed Gaussian for these calculations—and the values quoted are the root mean square which can be somewhat larger than, for example, the value of FWHM/2.355.

The bunch length limitation due to second order momentum compaction may be compensated, if necessary, by including a second harmonic *rf* section, immediately

adjacent to the first, at a decelerating phase to cancel the quadratic term in (18)[10]. Adding a compensating voltage V_c at a wavelength $\lambda_c=\lambda/2$ and a decelerating (cosine) phase, equation (18) becomes

$$z_1 \approx \alpha\delta_0 + \alpha_2 k^2 z_0^2 - \frac{2\pi^2 e V_c}{\lambda_c^2 E_0} z_0^2 \quad , \tag{29}$$

and the quadratic z_0 dependence is canceled by setting the compensating voltage to

$$V_c = -\frac{3eV_0^2\lambda_c^2}{E_0\lambda^2} \quad , \tag{30}$$

which is 8.2 MV (8.8 MV) in the TESLA (SBLC) design (no compensation is included in the design). The bunch length limitation due to sinusoidal rf may be compensated by designing for an appropriately smaller linear bunch length[4].

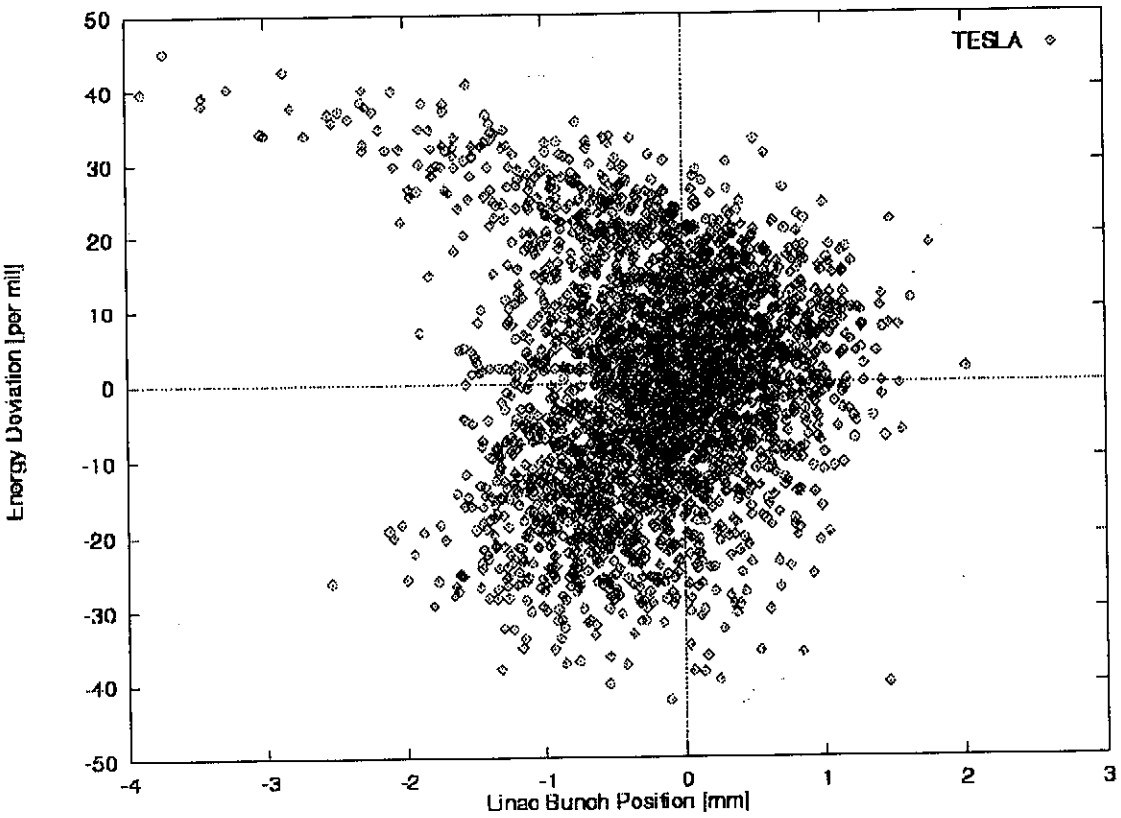

Fig 8. Longitudinal phase space at the main linac entrance after the complete TESLA bunch compressor beamline. The rms bunch length is 0.68 mm, the rms energy spread is 1.48 % and the *rf* voltage has been adjusted to minimize the bunch length (207 MV). The tracking was performed with 2nd order TURTLE[9], including sinusoidal *rf*, using 3000 Gaussian input rays with Table I rms values.

10 Compression with a 180° Arc

In the SBLC design, since it may be desirable to keep the two damping rings together, a 180° arc may be needed to turn the beam direction around. The use of the arc as a compressor may seem logical, however in order to provide the necessary (small)

momentum compaction, the arc length becomes long and the number of FODO cells becomes large. Table VII below summarizes the parameters for a 3.15 GeV arc for the SBLC in the first case as a compressor with $\alpha_a = -0.26$ mm and in the second case as a simple turnaround (*i.e.* α_a is allowed to increase and the *rf* section follows the arc rather than precedes it). In both cases the phase advance per cell of the arc is $\Delta\psi_x = 108^\circ$, $\Delta\psi_y = 90^\circ$ and the quadrupole bore radii are 8 mm with 8 kG pole tip fields and a 25 cm drift is maintained at each quadrupole.

Table VII. 180° arc parameters for SBLC as a bunch compressor and also as a simple turnaround.

parameter	symbol	unit	compressor	turnaround
momentum compaction of arc	α_a	meters	–0.26	–1.40
number of FODO cells	N_c	—	64	12
total arc length	L_{tot}	meters	160	36
SR x-emittance dilution	$\Delta\varepsilon_{SR}/\varepsilon_0$	%	0.004	2.0
maximum x-dispersion	η_{max}	mm	63	402
relative depolarization	$\langle P\rangle/P_0$	%	5.7	0.03

The non-compressor arc (turnaround) is much shorter and has <1/5 the number of FODO cells. Without the design constraint of $\alpha_a = -0.26$ mm the arc can be pushed to the synchrotron radiation limit of ~2% emittance increase. The high energy spread necessary in the compressor arc also depolarizes a transverse polarized electron beam by ~6%, tightens alignment tolerances and may introduce chromatic emittance dilution. Given these differences, if a turnaround is desirable, it is better to turn the beam around in a non-compressing arc (with the small damping ring energy spread) and then compress the bunch with an *rf* section followed by a wiggler. The longitudinal phase space is then only slightly affected. The bunch length relationship for the wiggler in (4) and (5) is unchanged and the linac energy spread in (6) becomes

$$\sigma_{\delta_1} = \sigma_{\delta_0}\sqrt{\left(\frac{\sigma_{z_0}}{\sigma_{z_1}}\right)^2 + \left(1 - \frac{\alpha_a}{\alpha_w}\right)^2} \quad . \tag{31}$$

This gives an upper limit to the arc momentum compaction, α_a, relative to the wiggler momentum compaction, α_w (note: $\alpha_a<0$ while $\alpha_w>0$). For the turnaround parameters of Table VII the energy spread is increased from the value of 1.53 % (in Table I) to 1.70 %. The energy-position correlation is changed from (7) to

$$r \equiv \frac{\langle z_1\delta_1\rangle}{\sigma_{z_1}\sigma_{\delta_1}} = \frac{\sigma_{\delta_0}}{\sigma_{\delta_1}}\left(1 - \frac{\alpha_a}{\alpha_w}\right) \quad , \tag{32}$$

which, from Table VII, gives a significant correlation of 0.43 at the linac entrance. An isochronous arc is also possible if the increased energy spread and correlation are too

large. In any case the arc design can be decoupled from the bunch compressor design as long as α_a is limited according to (31) and (32).

11 Conclusions

The bunch compressor beamline described includes a spin rotator system, skew correction section, bunch compression *rf*, a wiggler for path length energy dependence, phase space diagnostic for all six dimensions and several tuning elements for correction of errors. The tolerances of the system, when considering the correction available, are not difficult. A similarly detailed bunch compressor beamline for the SBLC can easily be derived with slight modifications to the optics (see Table II) and can be used for both electrons and positrons. If a turnaround is required for collider layout it should be designed as simply a beam turnaround and not a bunch compressor. The bunch compression can best be handled after the turnaround with the wiggler system described here.

12 Acknowledgments

I would like to extend my thanks to Michael Boege, Reinhard Brinkmann, Georg Hoffstaetter and Torsten Limberg and for many helpful discussions along the way. Furthermore, many of the ideas presented here were originally suggested by Tor Raubenheimer and Frank Zimmermann.

13 References

1. K. L. Brown *et al.*, CERN 80-04, March 1980.

2. R. Brinkmann, private communication (May, 1995).

3. T. O. Raubenheimer, P. Emma, S. Kheifets, *Chicane and Wiggler Based Bunch Compressors for Future Linear Colliders*, Proc. of the 1993 Particle Accelerator Conference, Washington, D.C., 1993.

4. The momentum compaction has been chosen slightly smaller than the linear design would require in order to somewhat compensate for *rf* non-linearities (see section 9).

5. P. Emma, *A Spin Rotator System for the NLC*, NLC-NOTE 7 (December, 1994).

6. T. Fieguth, *Snakes, Serpents, Rotators and the Octahedral Group*, SLAC-PUB-4195, January, 1987.

7. The term "wire scanner" may refer to a laser wire rather than a metallic filament, depending on survivability details. However, it will be prudent to include simple, well tested metallic filament type wire scanners for single bunch measurement to initially commission the beamline.

8. P. Emma, *A Skew Correction and Diagnostic Section for Linear Colliders*, NLC-NOTE in preparation.

9. D.C. Carey, et al., *Decay Turtle*, SLAC-246 (March 1982).

10. F. Zimmermann, *Longitudinal Single Bunch Dynamics and Synchrotron Radiation Effects in the Bunch Compressor*, NLC-Note 3, SLAC, October, 1994.

11. Georg Hoffstaetter, private communication (May 1995).

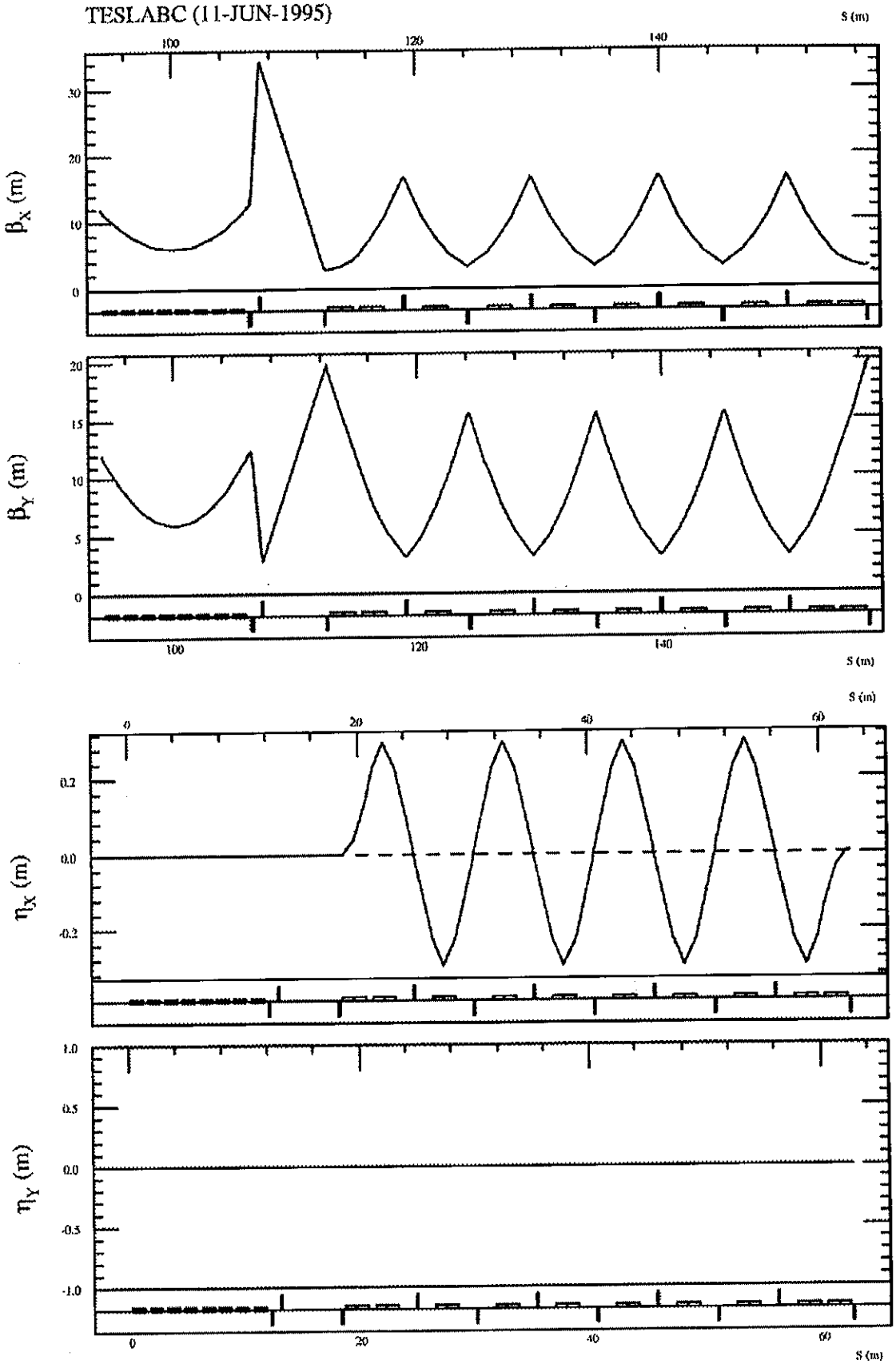

Fig. 1. Beta and dispersion functions for the TESLA wiggler and *rf* section. Dipole magnets are shown as low rectangles biased above the beamline while the eight *rf* structures are centered. Horizontal focusing quadrupoles are biased above while vertical focusing are biased below.

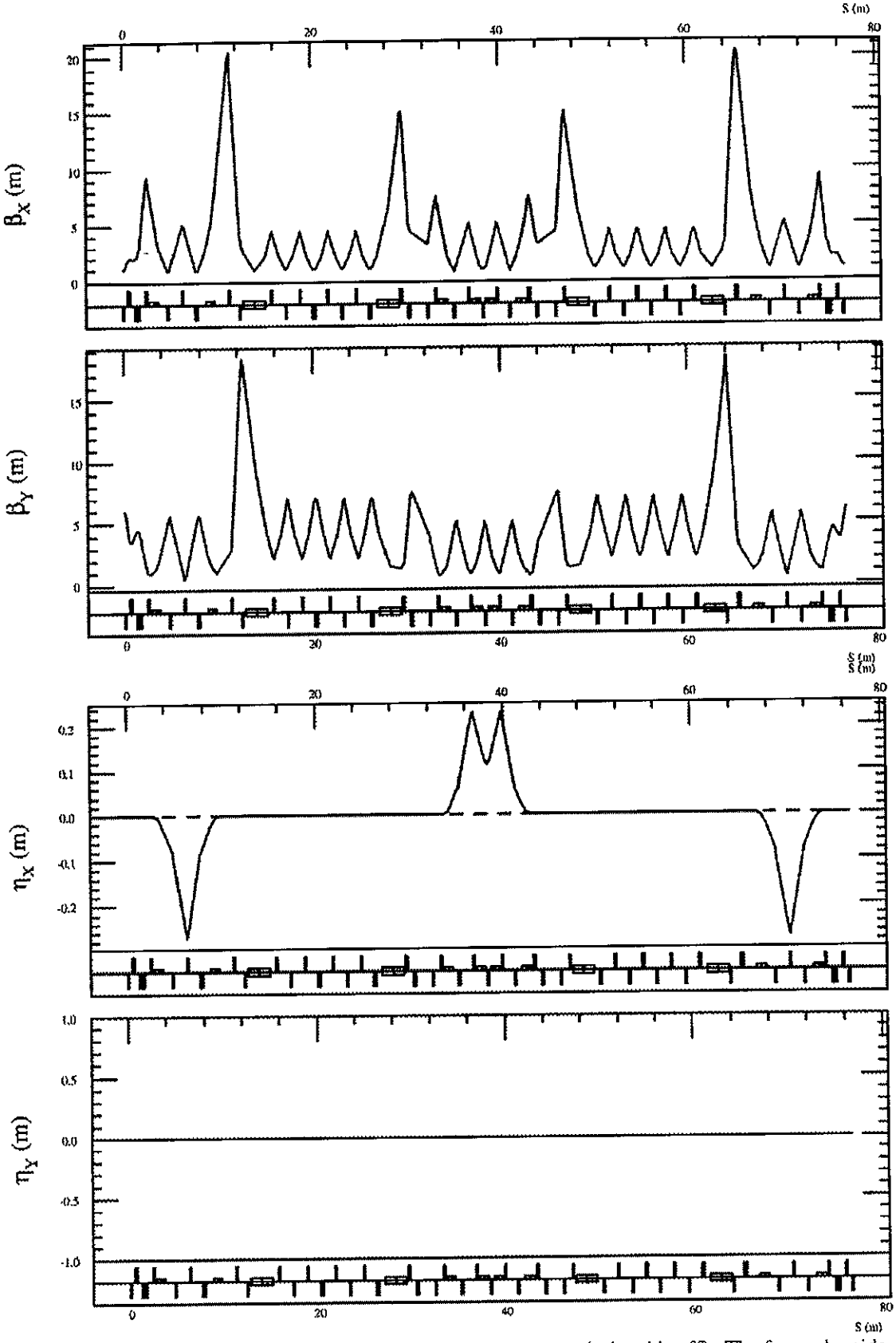

Fig 2. Beta and dispersion functions of the spin rotator system (solenoids off). The four solenoids are shown as long rectangles centered around the beamline. The two negative dispersion peaks are generated by two 6° arcs which, with the necessary central 12° arc, form a bump of 3.1 meters. The 6° arcs are only shown here for completion. They may be tailored to suit a specific DR extraction design.

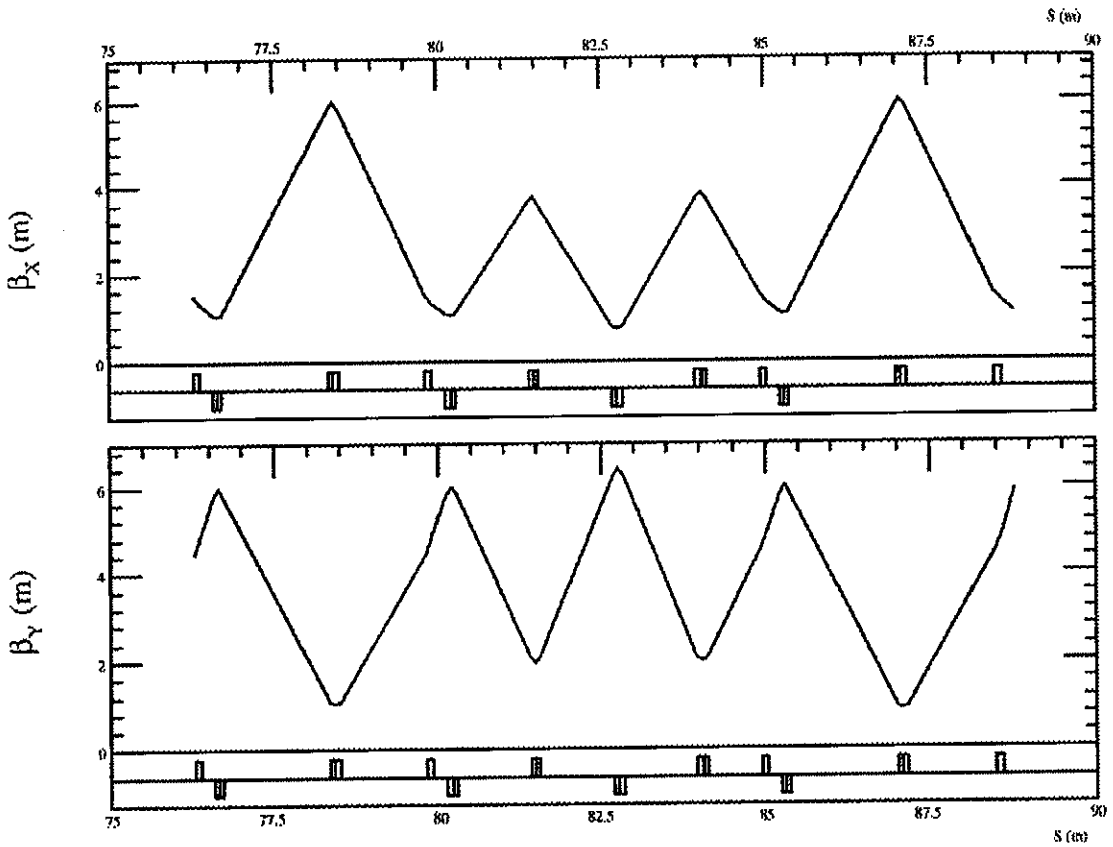

Fig. 3. Beta functions of skew correction section (SCS). The four skew quadrupoles are seen as the slightly narrower positive going rectangles each just upstream of vertically focusing quadrupoles.

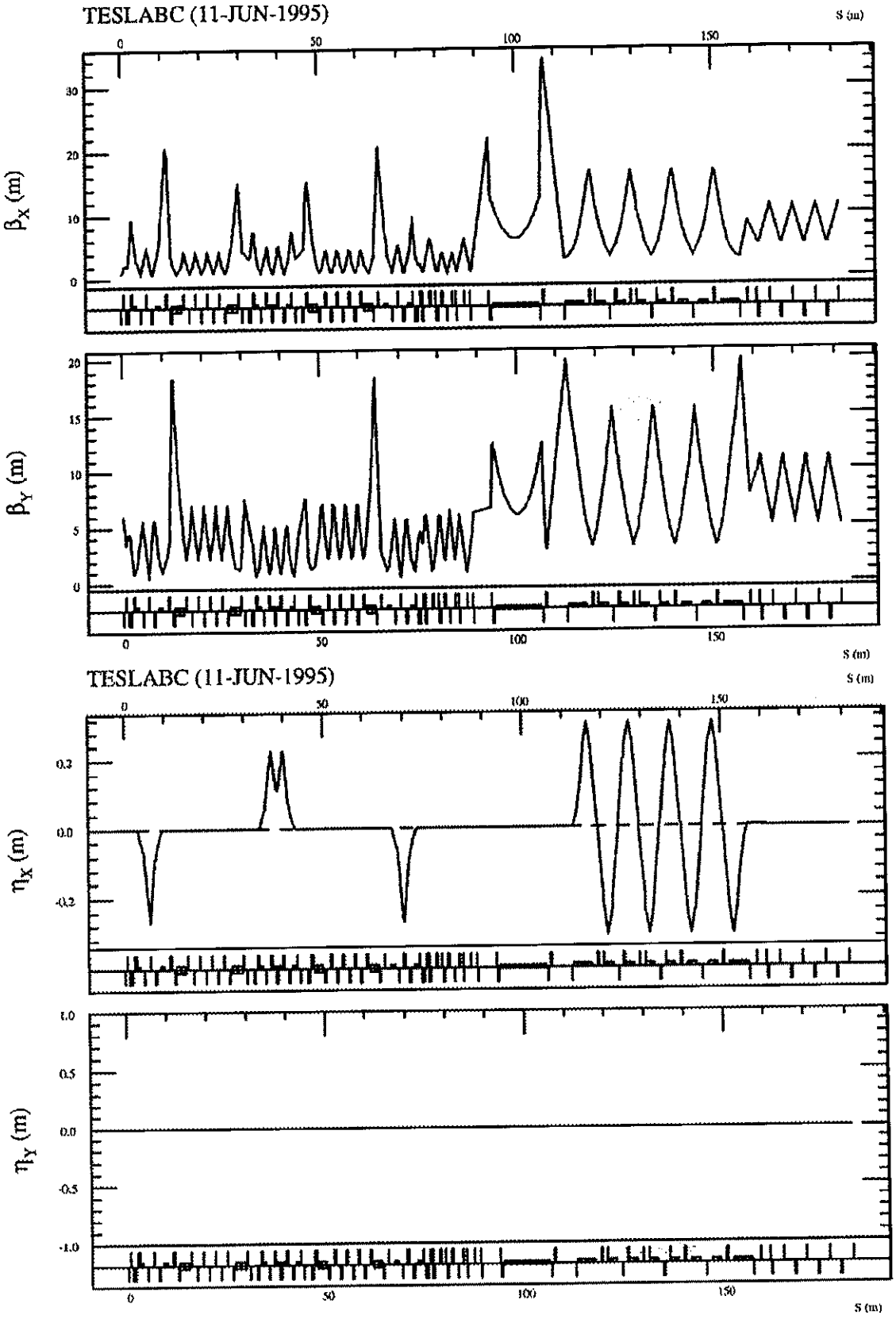

Fig. 4. Beta and dispersion functions of entire bunch compressor beamline—from spin rotator through diagnostic section (all solenoids off).